

Distribution of the SERS Enhancement Factor on the Surface of Metallic Nano-Particles

Walter R. C. Somerville, Baptiste Auguie, and Eric C. Le Ru

The MacDiarmid Institute for Advanced Materials and Nanotechnology, School of Chemical and Physical Sciences,
 Victoria University of Wellington, Wellington 6012, New Zealand

Email: walter.somerville@vuw.ac.nz, baptiste.auguie@vuw.ac.nz, eric.leru@vuw.ac.nz

Abstract—We discuss some theoretical investigations into the variation of the local-field enhancement factors on the surface of a variety of different experimentally-relevant particle geometries. We in particular examine the localization of the surface electromagnetic fields (hot-spots), and discuss some metrics that may be used to quantify this localization, and the hot-spot strength.

Index Terms—Near-field, Plasmonics, SERS

I. INTRODUCTION

The technique of surface-enhanced Raman scattering (SERS) [1]–[3] exploits electromagnetic enhancements near silver or gold nano-particles to dramatically increase Raman signals. These enhancement factors (EF) can be as large as 10^{10} , thereby allowing for single molecule (SM) detection under appropriate conditions [4]–[7]. Such large enhancements however only occur at highly localized positions on the metallic surface, so called hot-spots, for example, at the gap between two nano-particles [8]–[12] or at the tip of elongated particles [13]–[15]. Understanding how the EF varies in the vicinity of these hot-spots and the overall EF distribution [11] on the surface is therefore crucial to the understanding of SERS in general and SM-SERS in particular.

The enhancement factor, F , in SERS is mainly due to the electromagnetic enhancement arising from the metallic surfaces that the analyte is near. By virtue of optical reciprocity, the value of this enhancement is approximately [16] the product of the local field intensity enhancement, $(E/E_0)^2$, at both the laser and Raman wavelengths. We make the further approximation that this is $F \approx (E/E_0)^4$ for simplicity (this amounts to neglecting the Raman shift). Hence determining the enhancement factors requires solving for electric fields in the vicinity of the surface for the case of incident plane waves.

A variety of methods are used to solve the Maxwell equations based on the geometry being considered. For spheroidal particles, the Extended Boundary Condition Method (EBCM) and T-matrix method are used [14], [17] and provide an exact solution (including retardation/radiation effects). For more complex shapes, such as the bicones discussed later, we have used finite element modelling (COMSOL 4.1 software [18]) in the electrostatics approximation.

In all cases, we are concerned with surface fields at the main dipolar plasmon resonance (the most redshifted one), and for one orientation (with polarization along the long axis, where the field enhancements are largest).

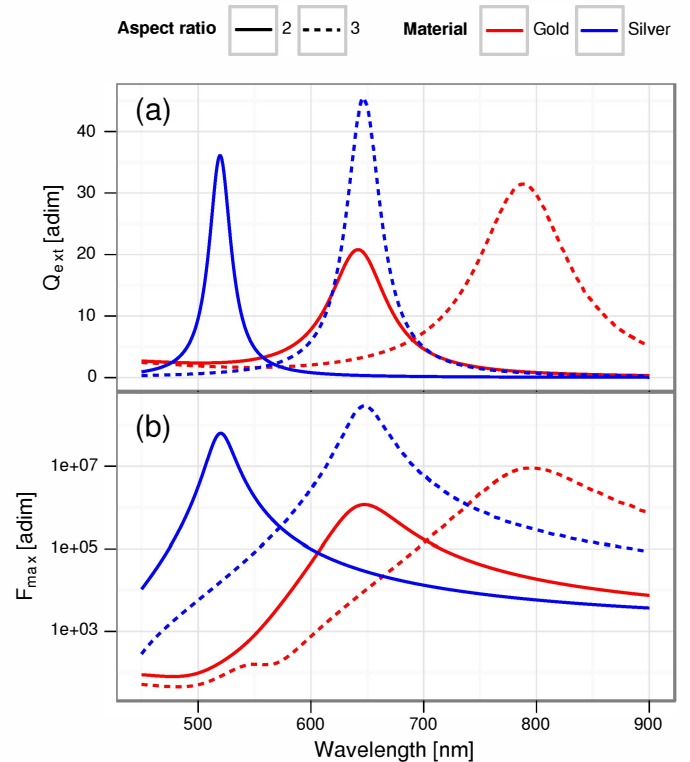


Fig. 1. A comparison of the resonance behaviour of various prolate spheroids when excited with the electric field parallel to the long axis. There are a selection of different spheroids considered, with some combination of different composition (gold, silver), aspect ratio ($h = 2, 3$), and minor-axis length (12.5nm, 25 nm). (a) presents the far-field spectra of the extinction coefficients for the cases considered. (b) shows the maximum enhancement factor found on the surface of the particle as a function of incident wavelength. We can see that the maximum enhancement factor follows the far-field behaviour

II. RESULTS

There are two uses of SERS that we might take an interest in, which have slightly different requirements [5]. The first is to increase the signal from a collection of molecules, where a large signal intensity, and thus a high average enhancement, is desired. The other is single molecule SERS. In this case, it is preferable to have a high degree of localization to the hot-spot, so that multiple molecules adsorbed on the surface away from the hot-spot do not contribute to the signal, but rather only molecules right at the hot-spot make a contribution, a situation

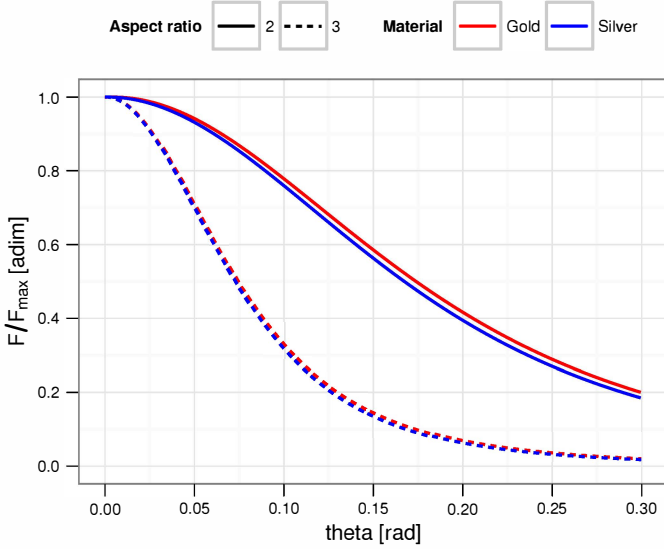


Fig. 2. Distribution of F/F_{\max} near to the hot-spot for a variety of different spheroids. Each of the two groupings of lines is two lines, of different materials. The difference between the two groupings is the aspect ratio (shape). In all cases the particles were examined at their dipolar plasmon resonance, and the values of F_{\max} varies between the particles, as seen in Fig. 1(b).

which can be probed experimentally with for example the bi-analyte SERS method [19].

Several different metrics are possible to consider properties of hot-spots. The ones that have been most studied are those relating to the magnitude of the enhancement factor, for example maximum EF at the hot-spot, F_{\max} or average EF on the particle, $\langle F \rangle$. Here we focus on the distribution of the EF around the hot-spot, rather than its amplitude. We study metrics that are not reliant on the maximum enhancement, but examine the hot-spot in the context of the particle that it is on.

The metrics that we use are modelled on those from [5]. The aim of these metrics is to characterize the *localization*, rather than the absolute strength (e.g. the maximum enhancement) of the hot-spot. This allows the localization of hot-spots on different particles to be compared. The metric $R = F_{\max}/\langle F \rangle$ is a measure of the strength of the hot-spot relative to the rest of the particle. This represents the number of analytes randomly positioned on the particle that would provide a SERS signal equivalent to the signal from one analyte at the hot-spot. A similar metric is the area from which a given proportion of the signal of randomly positioned analytes arises, a_p for some percentage p . Typically we use a_{80} . This, like R , provides a measure of how localized the hot spot is, in the context of that particle. Another possible approach is to study the EF distribution, that is how F/F_{\max} varies along the surface of the particle, moving away from the hot-spot. We parameterize this by angle, but arc-length is another possible parameterization. This provides a measure of how the enhancement factor is distributed on the surface of the particle, and how sharply the enhancement drops away from the maximum value.

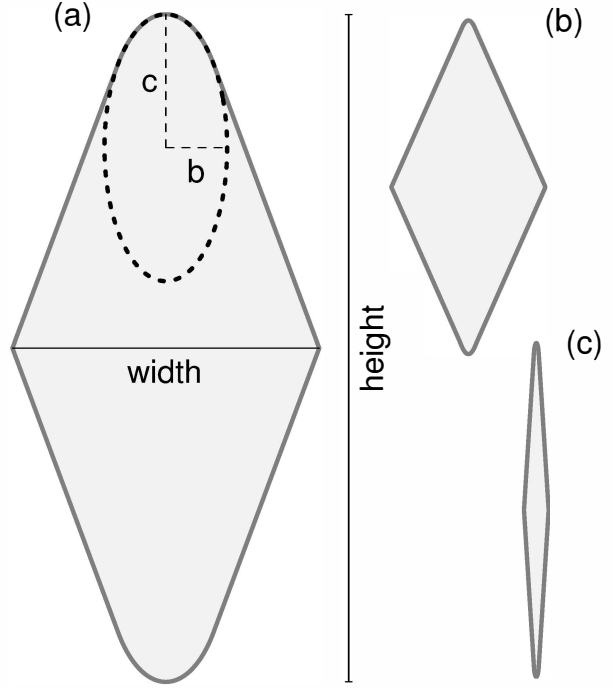
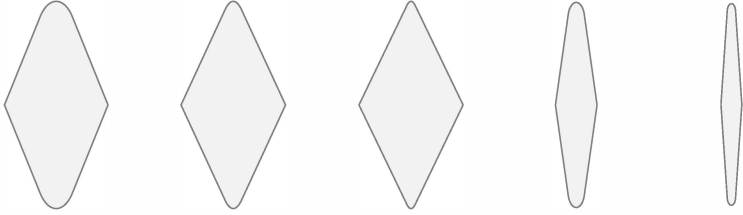


Fig. 3. Schematic of the bicone geometry. This provides both global shape parameters, width and height, and allows for the curvature at the spheroidal tips to be varied via the parameters b and c . (a) The shape considered is generated by rotating this shape around its long axis. The smaller figures demonstrate the effect of (b) changing the tip and (c) changing the overall aspect ratio, but leaving the tip unchanged.

A. Spheroid results

The use of these metrics leads to some interesting results. In the case of spheroids, the ratio at resonance of maximum to average enhancement factor, $R = F_{\max}/\langle F \rangle$, is a function of aspect ratio, independent of size, material, embedding medium [14]. In Fig. 2 we can see evidence of this. For several different spheroids, differing in aspect ratio, size, and composition, we examine the resonance behaviour. Fig. 1 shows the location of the resonances, of both the extinction coefficient, and the maximum value of F . We can see that these vary, as one would expect. However, in Fig. 2, we can see that the normalised enhancement distribution at resonance near the hot-spot for two spheroids of different size and material but the same aspect ratio is very similar. In contrast, for two spheroids of the same material, but a different shape, the angular dependence is clearly different, with the higher aspect ratio particles showing a higher degree of localization. This suggests that this distribution, F/F_{\max} , is a shape effect, independent of material. Additional studies also show that this is also independent of size. However, in this example, it is not obvious whether this distribution varies due to the local curvature at the hot-spot (where the electric field is strongest, due to the so-called “lightning-rod” effect), or due to the overall aspect ratio of

TABLE I
SUMMARY OF RESULTS FOR BICONES, FOR A SELECTION OF DIFFERENT GEOMETRIC PARAMETERS.



Aspect ratio h	2	2	2	5	10
Tip aspect ratio h_{tip}	2	5	10	2	2
F_{max}	1.93×10^8	6.69×10^9	7.65×10^{10}	4.49×10^9	4.29×10^9
$\langle F \rangle$	7.43×10^6	6.14×10^7	3.14×10^8	1.14×10^8	6.49×10^7
R	25.95	108.98	244.01	39.42	66.10
$\lambda(\text{nm})$	638	656	672	978	1546
a_{80}	8.33%	2.08%	0.726%	8.16%	6.55%

the particle.

For the spheroid, we are able to change two geometric parameters, the width and aspect ratio (alternatively height). However, as the localization (as demonstrated by the angular variation of F/F_{max} , or the ratio R) is independent of size [14], this leaves only the aspect ratio to change. Unfortunately, this affects both the global shape (i.e. aspect ratio) and the local geometry (for example characterized by the curvature at the tip). We cannot therefore identify with this class of particle shape which (local vs global geometry) is the main determining factor in the hot-spot localization effect (or equivalently EF distribution).

B. Rounded Bicone results

By examining rounded bicones, for which a schematic is provided in Fig. 3, we can attempt to disentangle the effects of overall shape and local shape on the hot-spot properties. Compared to a spheroid, where only the aspect ratio can be varied, the bicone offers an extra parameter, which allows investigation into the physical origin of localization. We are able to change the width and height of the bicone, thus altering the overall aspect ratio, while at the same time we can keep the local curvature at the tips constant, by keeping the spheroidal part of the tip the same. Conversely, we may alter the curvature of the tip, by changing the parameters of the spheroidal tip, while keeping the width and height of the bicone constant. This is demonstrated in Fig. 3, where the outline obtained by changing the tip properties is provided.

From these, we can elucidate the effect of local and global shape on the hot-spot localization. We find that the global shape has the most effect on the resonance wavelength, but it is the local shape that dictates the localization properties of the hot-spot. Since size effects are secondary to the problem of EF distribution, we can confine our study to small-size particles and therefore solve the problem in the electrostatics approximation. The bicones considered were modelled in COMSOL, and simulated using axiymmetric electrostatics. An example of the mesh used is given in Fig. 4(a), and the

enhancement factor in the vicinity of a particle at resonance is given in Fig. 4(b). The distribution of the enhancement factor on the surface at resonance near the hot-spot is provided in Fig. 4(c).

Various results for bicones are provided in Table I, for slightly different shape parameters. From these values we can examine the effect of geometric parameters on different properties. If we consider first the resonance wavelength, λ , we can see that this changes much more when the overall shape is changed, compared to when just the tip is changed. This is in line with expectations, that the resonance position is determined by (in addition to size and material) the overall particle aspect ratio, rather than the specifics of the particle shape [14], [20]. In contrast, the ratio R varies much more when the tip curvature is changed than when the overall shape changes. The same is true for a_{80} , and to a lesser extent for F_{max} and $\langle F \rangle$, though the latter two are not so interesting, as they do not (individually) describe the hot-spot localization effect. Thus, we can see that the properties which relate to the localization of the hot-spot are mostly determined by the description of the tip curvature, and not greatly affected by the overall aspect ratio of the particle.

III. CONCLUSIONS

This work confirms the accepted phenomenology that the plasmon resonance wavelength is primarily determined by particle shape, size and composition. It moreover extends it to the study of EF distribution at the resonance position (which are much more relevant to SERS experiments, in particular SM-SERS). We showed in particular that the hot-spot localization effect is primarily determined by the local curvature at the hot-spot, and not by the global geometry (aspect ratio). This work also highlights the remarkable sensitivity of properties like the maximum and average SERS EF at the hot-spot to minute changes in the particle geometry (see for example the first three shapes in Table I). This emphasizes the potential difficulty in correlating experimentally determined structural properties (for example measured from electron microscopy) to SERS performance [12], [21], even for single particles.

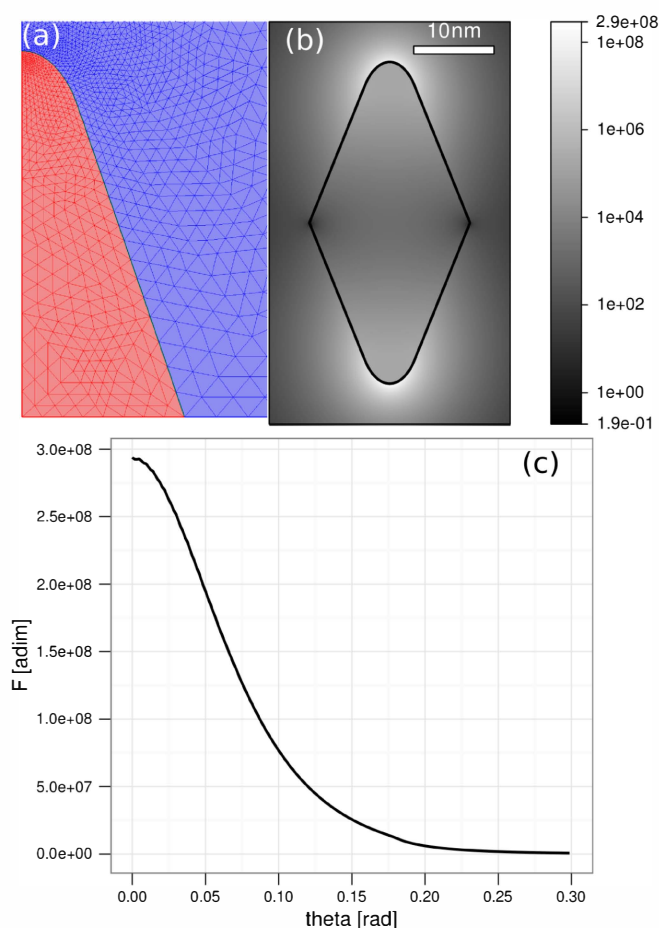


Fig. 4. (a) Demonstration of the mesh used in COMSOL for the bicone, for an electrostatic (axisymmetric) simulation. (b) A logscale map of the enhancement factor F in the vicinity of a bicone at resonance. (c) The angular variation of the enhancement factor on the surface of a bicone at resonance, near to the hot-spot.

The results of this work will nevertheless aid in the design of substrates for SERS, by providing information about which parts of the nanostructure critically affect the properties of hot-spots.

ACKNOWLEDGMENT

We are indebted to the Royal Society of New Zealand for funding through a Marsden Grant (WRCS and ECLR) and a Rutherford Discovery Fellowship (ECLR).

REFERENCES

[1] M. Moskovits, "Surface-enhanced spectroscopy," *Rev. Mod. Phys.*, vol. 57, no. 3, pp. 783–826, 1985.

[2] E. C. Le Ru and P. G. Etchegoin, *Principles of Surface Enhanced Raman Spectroscopy and Related Plasmonic Effects*. Amsterdam: Elsevier, 2009.

[3] R. F. Aroca, *Surface-Enhanced Vibrational Spectroscopy*. Chichester: John Wiley & Sons, 2006.

[4] E. C. Le Ru, E. Blackie, M. Meyer, and P. G. Etchegoin, "Surface enhanced Raman scattering enhancement factors: a comprehensive study," *J. Phys. Chem. C*, vol. 111, pp. 13794–13803, 2007.

[5] P. G. Etchegoin and E. C. Le Ru, "Single-Molecule SERS," *Annu. Rev. Phys. Chem.*, vol. 63, no. 1, 2012.

[6] N. P. W. Pieczonka and R. F. Aroca, "Single molecule analysis by surface-enhanced Raman scattering," *Chem. Soc. Rev.*, vol. 37, pp. 946–954, 2008.

[7] P. G. Etchegoin and E. C. Le Ru, "A perspective on single molecule SERS: current status and future challenges," *Phys. Chem. Chem. Phys.*, vol. 10, pp. 6079–6089, 2008.

[8] H. Xu, E. J. Bjerneld, M. Käll, and L. Börjesson, "Spectroscopy of single hemoglobin molecules by surface enhanced Raman scattering," *Phys. Rev. Lett.*, vol. 83, pp. 4357–4360, 1999.

[9] J. Jiang, K. Bosnick, M. Maillard, and L. Brus, "Single molecule Raman spectroscopy at the junctions of large Ag nanocrystals," *J. Phys. Chem. B*, vol. 107, no. 37, pp. 9964–9972, 2003.

[10] M. Futamata, Y. Maruyama, and M. Ishikawa, "Critical importance of the junction in touching Ag particles for single molecule sensitivity in SERS," *J. Mol. Structure (Theochem)*, vol. 735, no. Sp. Iss. S1, pp. 75–84, 2005.

[11] E. C. Le Ru, P. G. Etchegoin, and M. Meyer, "Enhancement factor distribution around a single surface-enhanced Raman scattering hot spot and its relation to single molecule detection," *J. Chem. Phys.*, vol. 125, no. 20, p. 204701, 2006.

[12] J. P. Camden, J. A. Dieringer, Y. Wang, D. J. Masiello, L. D. Marks, G. C. Schatz, and R. P. Van Duyne, "Probing the structure of single-molecule surface-enhanced Raman scattering hot spots," *J. Am. Chem. Soc.*, vol. 130, no. 38, pp. 12616–12617, 2008.

[13] P. W. Barber, R. K. Chang, and H. Massoudi, "Surface-enhanced electric intensities on large silver spheroids," *Phys. Rev. Lett.*, vol. 50, pp. 997–1000, 1983.

[14] R. Boyack and E. C. Le Ru, "Investigation of particle shape and size effects in SERS using T-matrix calculations," *Phys. Chem. Chem. Phys.*, vol. 11, pp. 7398–7405, 2009.

[15] E. C. Le Ru, J. Grand, I. Sow, W. R. C. Somerville, P. G. Etchegoin, M. Treguer-Delapierre, G. Charron, N. Flidj, G. Lvi, and J. Aubard, "A Scheme for Detecting Every Single Target Molecule with Surface-Enhanced Raman Spectroscopy," *Nano Lett.*, vol. 11, no. 11, pp. 5013–5019, 2011.

[16] E. C. Le Ru and P. G. Etchegoin, "Rigorous justification of the $|E|^4$ enhancement factor in Surface Enhanced Raman Spectroscopy," *Chem. Phys. Lett.*, vol. 423, no. 1, pp. 63–66, 2006.

[17] M. I. Mishchenko, L. D. Travis, and A. A. Lacis, *Scattering, absorption and emission of light by small particles*. Cambridge: Cambridge University Press, 3rd electronic release ed., 2002.

[18] "COMSOL AB." <http://www.comsol.com>, 2011.

[19] E. C. Le Ru, M. Meyer, and P. G. Etchegoin, "Proof of single-molecule sensitivity in surface enhanced Raman scattering (SERS) by means of a two-analyte technique," *J. Phys. Chem. B*, vol. 110, pp. 1944–1948, 2006.

[20] K. L. Kelly, E. Coronado, L. L. Zhao, and G. C. Schatz, "The optical properties of metal nanoparticles: the influence of size, shape, and dielectric environment," *J. Phys. Chem. B*, vol. 107, pp. 668–677, 2003.

[21] A.-I. Henry, J. M. Bingham, E. Ringe, L. D. Marks, G. C. Schatz, and R. P. Van Duyne, "Correlated structure and optical property studies of plasmonic nanoparticles," *J. Phys. Chem. C*, vol. 115, no. 19, pp. 9291–9305, 2011.